CSF1R and BTK inhibitions as novel strategies to disrupt the dialogue between mantle cell lymphoma and macrophages

Antonin Papin, Benoit Tessoulin, Céline Bellanger, Anne Moreau, Yannick Le Bris, Hervé Maisonneuve, Philippe Moreau, Cyrille Touzeau, Martine Amiot, Catherine Pellat-Deceunynck, et al.

CSF1R and BTK inhibitions as novel strategies to disrupt the dialogue between mantle cell lymphoma and macrophages

Antonin Papin[1,2,7], Benoit Tessoulin[1,3,7,‡], Céline Bellanger[1,2,7,‡], Anne Moreau[4,7], Yannick Le Bris[1,5,7], Hervé Maisonneuve[6,7], Philippe Moreau[1,3,7], Cyrille Touzeau[1,3,7], Martine Amiot[1,2,7], Catherine Pellat-Deceunynck[1,2,7], Steven Le Gouill[1,3,7,‡] and David Chiron[1,2, 7,‡,*]

[1]CRCINA, INSERM, CNRS, Université d'Angers, Université de Nantes, Nantes, France.
[2]GDR3697 Micronit, CNRS
[3]Service d'Hématologie Clinique, Unité d'Investigation Clinique, CHU, Nantes, France.
[4]Service d'Anatomie Pathologique, CHU, Nantes, France.
[5]Service d'Hématologie Biologique, CHU, Nantes, France
[6]Centre Hospitalier de la Roche sur Yon, Roche sur Yon, France.
[7]L'Héma-NexT, i-Site NexT, Nantes, France
[‡]Equal contribution

* Corresponding author:
Tel: +33 228080297
Address: 8 quai Moncousu, 44007 Nantes, France
E-mail: david.chiron@univ-nantes.fr

Running Title: MCL/macrophage protumoral interplay

Key words: CSF1, Lymphoma, CD163^{+} macrophages, ibrutinib

Disclosure

S. Le Gouill is a consultant/advisory board member and has received an honorarium from Roche and Janssen-Cilag. No potential conflicts of interest were disclosed by the other authors.

The manuscript contains 6 Figures, 8 supplementary figures and 2 supplementary tables

Abstract

The microenvironment strongly influences mantle cell lymphoma (MCL) survival, proliferation and chemoresistance. However, little is known regarding the molecular characterization of lymphoma niches. Here, we focused on the interplay between MCL cells and associated monocytes/macrophages. Using circulating MCL cells (n=58), we showed that, through the secretion of CSF1 and, to a lesser extent, IL-10, MCL polarized monocytes into specific CD163+ M2-like macrophages (MϕMCL). In turn, MϕMCL favored lymphoma survival and proliferation *ex vivo*. We next demonstrated that BTK inhibition abrogated CSF1 and IL-10 production in MCL cells leading to the inhibition of macrophage polarization and consequently resulting in the suppression of microenvironment-dependent MCL expansion. *In vivo,* we showed that CSF1 and IL-10 plasma concentrations were higher in MCL patients than in healthy donors, and that monocytes from MCL patients overexpressed CD163. Further analyses of serial samples from ibrutinib-treated patients (n=8) highlighted a rapid decrease of CSF1, IL-10 and CD163 in responsive patients. Finally, we showed that targeting the CSF1R abrogated MϕMCL-dependent MCL survival, irrespective of their sensitivity to ibrutinib. These data reinforced the role of the microenvironment in lymphoma and suggested that macrophages are a potential target for developing novel therapeutic strategies in MCL.

Introduction

Mantle cell lymphoma (MCL) is a rare and incurable B-cell malignancy, representing 3-10% of non-Hodgkin lymphomas (NHLs)(1,2). MCL cells are naive $CD19^+$ IgM^+ B-cells characterized by the expression of the B1-cell marker CD5 and the absence of CD23(3). Conventional MCL cells initially accumulate in the lymph nodes and disseminate early on into the peripheral blood or the bone marrow(4). In addition to the translocation t(11;14)(q13;q32), leading to the overexpression of Cyclin D1, conventional MCL cells are characterized by the overexpression of the oncogene SOX11. A SOX11-negative leukemic non-nodal MCL subtype is now well characterized and displays a limited number of genomic alterations, indolent clinical course, spleen involvement and a high percentage of circulating tumoral cells(5). Both subtypes can evolve into more aggressive forms (blastoid/pleomorphic) characterized by increased genomic instability and a high proliferation index(5). Several studies have described the nature of MCL genomic secondary alterations, such as frequent *ATM* or *TP53* mutations as well as recurrent copy number abnormalities and the deletion of *CDKN2A* or *TP53,* those being associated with a bad prognosis(6–8).

In addition to intrinsic tumoral abnormalities, the major role of the immune and stromal microenvironments in the expansion and chemoresistance of B-cell lymphomas is now widely accepted(9,10). MCL, one of the most aggressive B-cell lymphomas, does not escape this logic, and several studies have recently confirmed the role of the microenvironment in the survival, proliferation and chemoresistance of this NHL(11–16). Nevertheless, the composition of the MCL microenvironment and the resulting interactions that occur in the tumor niches remain largely unknown.

Among accessory cells, tumor-associated macrophages are known to play a critical role in solid tumor progression(17,18) and have also been described in several B-cell malignancies(19–22). Previous studies suggested the presence of macrophages in MCL lymph nodes(23,24) but their phenotype and the molecular dialogue that occurs between MCL cells and associated macrophages remain unknown.

In the present work, we have studied the dynamic interactions between MCL and its myeloid microenvironment. Using primary co-culture models *ex vivo,* we have demonstrated that primary MCL cells polarize monocytes into specific associated macrophages (M**ϕ**MCL), which support MCL growth and survival. Furthermore, we identified mechanism-based targeted strategies that disrupt the dialogue between MCL and M**ϕ**MCL *ex vivo* and *in vivo.*

Methods

Culture and co-culture of primary cells

Primary MCL cells were obtained after informed consent from patients according to protocols approved by local institutional review boards (REFRACT-LYMA cohort; ethical approval GNEGS-2015-09-13(25)) and in accordance with the Declaration of Helsinki. Patients' characteristics are summarized in the supplemental Table S1. Briefly samples from 58 patients (69% male; median age, 70 years) were used in this study, 61% at diagnosis and representing the different subtypes of the disease (37 conventional, 10 blastoid/pleomorphic, 9 leukemic non-nodal). Peripheral blood (PB) MCL cells were isolated after Ficoll-Hypaque separation and stored in liquid nitrogen. PB MCL cells (median of circulating cells, 50%) were separated from other mononuclear cells using anti-human CD19-conjugated magnetic beads (Miltenyi, Paris, France) with purity > 90%. For autologous cocultures, monocytes from patient were isolated using anti CD14-conjugated magnetic beads (Miltenyi, Paris, France). For allogeneic coculture experiments, PB primary monocytes from healthy donors were obtained by elutriation (CIC Biotherapy 0503, Nantes, France). For IL-10, CSF1 plasma concentrations and CD163 expression on monocytes, PB was obtained from age-matched (>60 years) healthy donors. Samples used for *in vitro* co-cultures or molecular characterisations were listed in Table S1.

For *in vitro* generation of classically activated M1 and alternatively activated M2 macrophages, monocytes were differentiated with CSF2 (GM-CSF, 20 ng/ml, 5 days) or CSF1 (M-CSF, 50 ng/ml, 5 days) before activation with IFNγ (10 ng/ml, 2 days) or IL-10 (25 ng/ml, 2 days), respectively (26,27).

$CD19^+$ primary MCL cells were cultured at 10^6 cells/ml alone or with monocytes or *in vitro* pre-differentiated macrophages at 2.10^5 cells/ml (5:1 ratio). Transwell assays were realized with a 0.4 µm pore polycarbonate membrane and 6.5 mm inserts (Corning, NY, USA). After co-cultures, MCL cells were separated from macrophages by removal of non-adherent cells and identified using B-cell markers by flow cytometry (CD19, CD20). Adherent macrophages

were detached using PBS-EDTA 0,02% (15 minutes at 4°C). All cells were maintained in RPMI-1640 medium (Gibco) supplemented with 10% fetal calf serum and 2mM glutamine.

Mantle cell lymphoma cell lines

JeKo-1, MINO, REC-1, MAVER-1 and GRANTA-519 were purchased from DSMZ (Braunschweig, Germany) and Z138 from ATCC (Manassas, USA). UPN1 and SP53 were kindly provided by Dr. V. Ribrag (Institut Gustave Roussy Villejuif, France) and Pr. S. Chen-Kiang (Cornell University, NY) respectively. NTS-3 and NTS-4 has been generated in our laboratory (CRCINA)(12). Cell lines are routinely identified using a flow cytometry–based barcode as previously described(28) as well as MHC class I sequencing and are tested for mycoplasma contamination. Values for MCL cell lines are the mean of at least 3 independent experiments.

Bioinformatics analysis

For mRNA relative expression level, CD19+ peripheral blood B cells from healthy donors (Normal B Cell, NBC, n = 15), MCL cells (n = 183) and myeloid cells (Monocytes, n = 6; MϕMCL, n = 4; M1, n = 3; M2, n = 5) datasets were collected from the GEO database (GSE50006, GSE19243, GSE35426, GSE16455, GSE36000, GSE21452, GSE70910, GSE76803, GSE28490, GSE124931, GSE95405, GSE20484). In order to overcome data normalization biases, only Affimetrix Human Genome U133 Plus 2.0 series with raw data were retained. Briefly, raw .CEL files were downloaded and processed in R-3.5.1 using the affy package, optical noise/background correction was performed by MAS5.0 or gcrma with standard options, expression batches were finally normalized by quantiles using the limma package(29,30). Principal Component Analysis was performed by FactoMineR and factoextra packages. A hierarchical ascendant clustering was performed using Euclidean distances and Ward.D2 method. Heatmap and radarchart were carried out with the ComplexHeatmap and fmsb package, respectively.

For deconvolution analysis of tumor bulk gene expression data (LN MCL, n=161, GSE16455, GSE93291, GSE16024, GSE36000, GSE70910) we used the Cibersort program (31). CD19+ sorted MCL cells from 4 LN (GSE70910) were used as an internal control for the deconvolution analysis.

Other Methods.

Cell cycle and viability assays as well as real-time quantitative reverse transcription polymerase chain reaction (qRT-PCR, control gene *RPL37A*) and Immunoblot protocols have been previously described(15). Antibodies and reagents are detailed in supplemental Table S2. Statistical analyses were performed using two-sided Mann Whitney, Wilcoxon matched-pairs signed-rank or t-tests as stated in the figure legends. Analyses were performed using GraphPad Prism and R statistical softwares and all tests were considered statistically significant at $p < .05$.

Results

Monocyte-derived macrophages support primary MCL cell survival and proliferation.

Using a deconvolution algorithm for tumor bulk gene expression data(31), we first observed that MCL lymph nodes (LN) were characterized by macrophage infiltration (median, 12%, n=161, Figure S1A). CD68+ macrophages were also highlighted in MCL LN by IHC (n=10), arguing for a potential dialogue between MCL and its myeloid microenvironment *in vivo* (Figure S1B).

To understand the potential role of this interplay, we first set up an *ex vivo* co-culture of peripheral blood primary MCL cells (PB MCL cells) and monocytes isolated from healthy donors. After 7 days of co-culture, we observed that monocytes differentiated into adherent macrophages (Figure S1C), which we called MCL-associated-macrophages (M**ϕ**MCL) throughout this study. PB MCL cells poorly survived when cultured alone. In contrast, the presence of monocytes greatly improved their survival after 7 days *ex vivo* (median Annexin-V^{neg}; alone, 6.5%; co-culture, 85.9%; n= 17; $p<0.001$; Figure 1A). The pro-survival advantage of the co-culture, observed as early as 48h, was maintained for several weeks and after several months of culture, the t(11;14) EBV^{neg} MCL cell line NTS4 (from sample 2b) remained dependent on M**ϕ**MCL for survival (data not shown). Using culture inserts to avoid contact between the two cell types, we determined that the pro-survival impact of monocytes was partly dependent on soluble factors (median survival alone, 5%; co-culture, 32.9%; $p<0.001$; Figure 1A). Indeed, whereas direct contact with monocytes induced a 13-fold increase of PB MCL cell survival, soluble factors supported a 6.5-fold survival increase (Figure 1A).

We have previously shown that in contrast to lymph node MCL cells, circulating MCL cells rarely proliferate (Figure S2A)(12). Here, we have demonstrated that monocyte co-culture supported the proliferation of primary MCL cells in 8/16 samples tested (median $BrdU^+$ cells in co-culture, 14.75%; Figure 1B, S2B), confirming the microenvironment-dependent expansion of MCL cells. Of note, monocyte-dependent proliferation was significantly lower in leukemic non-nodal (light grey bars, n=5) compared to conventional (dark grey bars, n=7) or

aggressive (black bars; n=4) MCL subtypes ($p<0.05$, Figure 1B). This monocyte-dependent increase in proliferation was confirmed at the molecular level by the induction of *MKI67* expression and the inhibition of the tumor suppressor Rb (ratio phospho (p)Rb/Rb) (Figure S2C-D). As observed for survival, cell cycle induction was, at least, partly dependent on soluble factors (Figure S2E). Of note, autologous monocytes/MCL cocultures displayed similar results (n=4, autologous vs. allogeneic coculture $p>0.35$, Figure 1C).

MϕMCL are M2-like macrophages.

In order to better characterize the interplay between MCL and its myeloid microenvironment, co-cultures of PB MCL cells in contact with *in vitro* pre-differentiated, classically activated (M1) or alternatively activated (M2) macrophages were set up. Even though M1 macrophages display anti-tumoral activities in several models, both M1 and M2 macrophages provided a similar pro-survival benefit to PB MCL cells (Figure S3A). As observed for monocytes, this pro-tumoral effect was, at least, partly due to soluble factors (Figure S3B), suggesting that both M1 and M2 macrophages secrete MCL pro-survival factors. Of note, M2 macrophages induced significantly more proliferation in PB MCL cells compared to M1 macrophages (median with M1 = 3%, with M2 = 9%, $p< 0.01$; Figure S3C).

To define the precise nature of MCL-associated-macrophages (M**ϕ**MCL) we analyzed their transcriptome along with the one of undifferentiated monocytes, M1 and M2 macrophages. To compare the different groups, we performed a Principal Component Analysis (PCA), and observed that M**ϕ**MCL segregated with M2 macrophages (Figure S4A). Accordingly, hierarchical clustering based on 17256 genes highlighted greater similarities of M**ϕ**MCL with alternatively activated M2 macrophages (Figure 2A).

Previously defined genes signatures allowed the robust prediction of monocytes, M1-like or M2-like phenotypes (Figure S4B)(31). It is noteworthy that *ex vivo* generated M**ϕ**MCL and macrophages infiltrated in MCL lymph nodes *in vivo* displayed a similar CSF1-differentiated M2-like macrophage signature (Figure 2B). In line with an M2-like profile, M**ϕ**MCL were characterized by the expression of the M2-like marker CD163, even though at a lower level

than *in vitro* pre-differentiated M2 macrophages (Figure 2C, S4C). MϕMCL arising from allogeneic or autologous CD14+ monocytes displayed a similar phenotype (Figure S4C) and the presence of CD163+ cells was confirmed in MCL LN by IHC or cytometry (Figure S4D-E). Given the key role of soluble factors in MϕMCL/MCL interplay (Figure 1), we analyzed the expression profile of genes coding for cytokines (n=24) and chemokines (n=28) in MϕMCL (Figure S4F). Even though hierarchical clustering based on these 52 genes highlighted greater similarities with M2 macrophages (Figure S4G), PCA demonstrated that MϕMCL formed a specific subtype of macrophages, producing both M2 and M1 associated factors (Figure S4H). Among them, the expression of known pro-tumoral cytokines in MCL such as IGF1, IL10 and IL6 (32–34) were confirmed in additional MϕMCL samples (n = 5, Figure 2C).

MCL cells secrete the M2 polarizing factors IL-10 and CSF1.

To determine how primary MCL cells polarized monocytes into specific CD163+ M2-like MϕMCL, the expression of known macrophage-polarizing factors(35) was analyzed. We first interrogated publicly available gene expression datasets and observed that *CSF1* and *IL10* transcripts, in contrast to *CSF2*, *IL4*, *IL34* or *IL13 (data not shown)*, were significantly overexpressed in MCL samples *in vivo,* when compared to normal B cells (NBC)(Figure 3A). Of note, *CSF1* but not *IL10* expression was significantly higher in MCL LN compared to MCL PB (Figure S5A). To confirm that these soluble factors were indeed produced by MCL cells, we assessed their expression in MCL cell lines (n=9) and purified PB MCL cells (n=20) by RT-qPCR (Figure 3B-C). Whereas only 3/9 cell lines (JeKo, Mino, Granta) co-expressed *CSF1* and *IL10*, transcripts for both factors were detected in 19 out of 20 primary MCL samples. *CSF1,* but not *IL10* mRNA, was significantly overexpressed in aggressive (blastoid/pleomorphic) MCL subtypes and correlated with proliferation in co-culture *ex vivo* ($BrdU^+$ cells in co-culture) and in tissues *in vivo* (*MKI67*) (Figure S5B-D). IL-10 (7/10) and CSF1 (7/10) expressions were then confirmed at the protein level in the MCL/MϕMCL co-culture supernatant (D7), with all samples tested secreting detectable amounts of at least one of both the factors (median CSF1, 4.35 pg/mL; median IL-10, 5.67 pg/mL)(Figure 3D).

To understand the role of the CSF1 and IL-10 in the initiation of MCL/monocyte interplay, we cultured monocytes with previously generated MCL/monocyte co-culture supernatants (7 days) in the presence of inhibitors of the CSF1R (GW2580 (36–38), blocking antibodies) or IL10R (blocking antibodies). We demonstrated that inhibition of the CSF1R significantly reduced monocyte survival (median viability reduction of 80% with GW2580, of 44% with anti-CSF1R, n= 6, Figure 3E). Inhibition of CSF1R with GW2580 significantly reduced the M2-like marker CD163 on remaining viable monocytes (median CD163 reduction of 45%, n= 5) (Figure 3E). Significant inhibition was also observed with anti-CSF1R monoclonal antibodies (median reduction of 28%, n= 5). Inhibition of IL-10R resulted in a slight, but not significant, reduction of the CD163 level on MϕMCL (median reduction of 16%, n= 5, Figure 3E). These data showed that MCL-secreted CSF1, but not IL-10, was essential for initiating the dialogue between MCL and monocytes.

In addition to inhibiting monocytes survival and polarization, CSF1R neutralization resulted in the inhibition of monocyte-dependent survival in all primary MCL samples tested (Figure 3F) (median monocyte-dependent survival reduction by GW2580 of 91%). Besides, we observed that CSF1R inhibition also resulted in an inhibition of primary MCL cells viability as well as a downregulation of macrophages CD163 expression in coculture experiments with pre-differentiated MϕMCL and M2, but not M1, macrophages (Figure S6A).

In accordance with the absence of CSF1R expression on MCL cells (data not shown), GW2580 did not display any direct cytotoxicity on primary MCL cells (Figure S6B), confirming that the loss of viability was the consequence of the inhibition of MCL/MϕMCL interplay. In addition, CSF1R inhibition with other inhibitors such as BLZ945 (37), the clinically available PLX3397 or anti-CSF1R mAb confirmed the results obtained with GW2580 (Figure S6C).

Taken together, the results showed that MCL cells secrete the M2-polarizing factors IL-10 and CSF1, the latter being essential for the initiation of the pro-tumoral dialogue between malignant B-cells and associated macrophages.

Ibrutinib disrupts the dialogue with MϕMCL by inhibiting MCL-specific CSF1 and IL-10 secretion.

Previous studies reported modulations of the MCL secretome, including IL-10, upon BTK inhibition with ibrutinib, both *in vitro*(39) and *in vivo*(40). To study the modulation of IL-10 and CSF1 upon ibrutinib treatment, Mino and Granta cell lines, which produce both factors, were first used (Figure 3B). As previously reported(41), it was confirmed that, in contrast to Mino cells, Granta was resistant to both cytotoxic and cytostatic ibrutinib effects *in vitro* (0.5 µM; data not shown). Both *CSF1* and *IL10* mRNA where dramatically reduced after 72h of ibrutinib treatment (0.5 µM) in the ibrutinib-sensitive Mino cells whereas no modulation was observed in the ibrutinib-resistant Granta cells (Figure 4A). These modulations were confirmed at the protein level using ELISA (Figure 4B). Of note, we observed an induction of the CSF1 expression in cell lines with a low baseline level (UPN1, JeKo) after BCR activation upon anti-IgM stimulation, confirming that CSF1 is a direct target of the BCR signaling network (Figure S7A).

In accordance with production of M2-polarizing factors, the co-culture of both cell lines induced CD163 expression on PB primary monocytes from healthy donors (Figure 4C). As expected, ibrutinib inhibited the M2-like polarization exclusively with the ibrutinib-sensitive Mino cells (mean reduction of 43%, n=3, Figure 4C). Taken together, the results suggested that ibrutinib treatment counteracted CD163+ MϕMCL polarization through inhibition of MCL-specific IL-10 and CSF1 secretion.

In addition to impairing MϕMCL polarization, ibrutinib treatment resulted in the inhibition of MϕMCL-dependent pro-survival and proliferative effects in 8 out of 14 and 4 out of 4 samples, respectively ($p<0.01$) (Figure 4D-E). Even though BCR signaling was constitutively activated, independently of monocyte coculture (Figure S7B), ibrutinib did not induce any cytotoxicity in primary MCL cells cultured alone *ex vivo* (Figure S7C). Besides, ibrutinib did not induce any cytotoxicity in monocytes/macrophages alone (data not shown). Thus, given that BCR inhibition abrogated MCL survival in coculture, it appears that ibrutinib acted mainly through the disruption of the interplay between tumoral cells and MϕMCL.

Early *in vivo* CD163 modulation on PB monocytes is observed upon ibrutinib treatment of MCL patients.

In accordance with the ability of primary MCL cells to produce CSF1 and IL-10, a significantly higher level of these M2-polarizing factors was detected in the plasma of MCL patients compared to age-matched healthy donors (HD) (median HD IL-10, 0pg/mL; CSF1, 0pg/mL; n= 9; median MCL IL-10, 1.2pg/mL; CSF1, 5.6pg/mL; n=28, Figure 5A). Likewise, CD163 was overexpressed at the surface of CD14+ PB monocytes in several MCL samples compared to healthy donors (median CD163 MFIr HD = 4.3, n=8; MCL= 7.5, n=32, Figure 5A), which was consistent with the CD163-inducing properties of CSF1 and IL-10. There was no significant correlation between the level of IL-10, CSF1 nor CD163 and the status of the disease (Diagnosis/Relapse).

We next evaluated IL-10 and CSF1 plasma concentrations as well as CD163 expression on CD14+ PB monocytes in 8 patients treated by anti-CD20 monoclonal antibody (Obinutuzumab) in combination with ibrutinib (protocol detailed in Figure S8A). PB samples were collected before (D0) and after 8 days of treatment (D8). IL-10 or CSF1 concentration was decreased at D8 in 8/8 and 2/3 evaluable plasma samples, respectively (IL10, n=8, $p<0.01$) (Figure 5B). In addition, CD163 expression on CD14+ PB monocytes was decreased in 7 out of 8 patients at D8 (median CD163+ reduction of 58%, n=7, $p<0.05$, Figure 5B). In contrast to ibrutinib (Figure 4A), the anti-CD20 mAb Obinutuzumab did not directly modulate *IL10* or *CSF1 in vitro* (Figure S8B).

The follow up of patients treated with anti-CD20 mAb and ibrutinib for several cycles (Pt# A1, A2, A5, A9) revealed that CD163 inhibition was durable and associated with a clinical response (>2 years) (Figure S8C). In fact, whereas the three patients characterized by a dramatic reduction in CD163 at D8 (Pt# A1, A2, A5) achieved a durable complete response, Pt# A9, who displayed an increase in CD163 expression and a limited decrease of IL-10 plasma concentration, progressed under treatment. Taken together, our retrospective analysis suggested that CD163 modulation upon ibrutinib treatment is associated with a

clinical response. These results warrant further investigation with a larger cohort of ibrutinib-treated patients.

CSF1R inhibition as an alternative for disrupting MCL/MϕMCL dialogue in ibrutinib-resistant patients

Ibrutinib did not efficiently counteract MϕMCL-dependent MCL survival in 6 out of 14 samples (Figure 4D), including two patients who previously demonstrated ibrutinib resistance *in vivo* (Pt#2 and #12). To assess whether alternative strategies targeting the MCL/MϕMCL dialogue could bypass ibrutinib resistance, the CSF1R inhibitor GW2580 was tested in both ibrutinib-sensitive (Pt#7, 11, 15, 16) and resistant (Pt#2, 5, 18, 19) primary cells. We showed that GW2580 reduced MCL cell viability in all samples tested, irrespective of their sensitivity to ibrutinib (Figure 6A), suggesting that targeting the CSF1/CSF1R axis could be of major interest in ibrutinib-resistant patients. To assess whether the association of BTK and CSF1R inhibitors could also be beneficial for ibrutinib-sensitive patients, the efficacy of ibrutinib/GW2580 combination was tested at lower concentrations (125 nM). We showed additive (Pt#11 and #47) or supra-additive (Pt#7 and #15) effects of the combination in ibrutinib-sensitive samples ($n= 4$, $p<0.05$, Figure 6B, left) but not in ibrutinib-resistant samples ($n= 4$, Figure 6B, right).

Discussion

Several studies have highlighted the central role of the microenvironment in the expansion and chemoresistance of B-cell lymphomas, including MCL(11–16,42). The few works that have examined the role of macrophages in MCL suggested a protumoral function(23,24), especially through the induction of a VEGF-dependent lymphangiogenesis (24). However little was known about the molecular interplay between MCL cells and associated monocytes/macrophages. Here we showed that, through secretion of IL-10 and CSF1, MCL polarizes monocytes into M2-like macrophages, which in turn favor tumor survival and proliferation.

IL-10 production by MCL cells has been previously reported *in vitro* and *in vivo*(39,40). In contrast, this is, to our knowledge, the first study reporting a CSF1 paracrine loop in MCL. CSF1 and IL-10 are involved in monocyte polarization into alternatively activated M2-like tumor-associated macrophages (TAM)(43). In addition, CSF1 and its receptor CSF1R are central to myeloid cell biology and promote migration, survival, and proliferation of monocytes(44). It is noteworthy that both *ex vivo* generated MΦMCL and *in vivo* MCL-infiltrated macrophages displayed a M2-like signature close to macrophages differentiated by the CSF1 (Figure 2B, S4B), highlighting the relevance of our *ex vivo* coculture model and reinforcing the key role of the CSF1 in MCL/monocyte interplay.

CSF1 production has been reported in several solid tumor models and has been associated with a poor prognosis(45,46). Regarding B-cell malignancies, *CSF1* transcript overexpression correlated with chronic lymphocytic leukemia (CLL) progression, however, CSF1 protein was not detected in the plasma of CLL patients(47). In our study, and using the same technology (ELISA), we detected a significant amount of CSF1 protein in 17 out of 28 MCL plasmas studied, highlighting a high production in MCL (Figure 5). In addition, we showed that *CSF1* was more expressed in the most aggressive forms of MCL and was associated with primary MCL cells proliferation (BrdU+) *ex vivo*. This was reinforced by a positive correlation between *CSF1* and *MKI67* (proliferation index) expression *in vivo* (GEP

analysis, n=183) and suggested an association between MCL/ MϕMCL interplay and tumor aggressiveness (Figure S5).

Even though transcriptome analysis showed that MCL associated-macrophages (MϕMCL) shared more similarities with M2 macrophages (Figure 2), M**ϕ**MCL expressed both M1 and M2-associated soluble factors (Figure S4F-H). This reflected the phenotypic and functional plasticity of macrophages polarization and suggested that additional factors to IL-10 and CSF-1 might be involved in MϕMCL polarization. Besides soluble factors, cellular contacts might also play a role in MCL/MϕMCL interplay. We observed that MϕMCL displayed a specific immune checkpoints profile and expressed both PD1 and PDL1 (Figure S4F), suggesting that immune checkpoint inhibitors could be of interest as another therapeutic avenue in MCL.

Given the central role of the myeloid microenvironment in numerous solid and hematological malignancies, several targeted strategies are under investigation. Among them, the CSF2-dependent re-education of M2-like TAM into classically activated anti-tumoral M1 macrophages has been proposed in several models such as glioblastoma or multiple myeloma(48,49). However, based on our *ex vivo* data, M1 macrophages could also provide pro-survival signal in MCL. The depletion of tumor-associated macrophages using targeted therapies has therefore appeared to be more attractive in MCL. Accordingly, we demonstrated that targeting the CSF1R using the small molecule GW2580 efficiently counteracted MϕMCL protumoral effects *ex vivo* (Figures 3,6). GW2580 is an orally bioavailable and selective CSF1R kinase inhibitor whose efficacy and selectivity have been previously demonstrated in different models (36–38,50,51). In addition, potential off target effects have been ruled out using other well described selective small molecules such as PLX3397 or BLZ945 as well as anti-CSF1R mAb. Success of such a strategy has been recently confirmed *in vivo* using clodrolip or anti-CSF1R mAb in a CLL mouse model(22). In humans, several anti-CSF1R mAb (LY3022855, Emactuzumab, AMG820) and CSF1R inhibitors (PLX3397, Pexidartinib) are currently being evaluated in phase I/II clinical studies that will soon document the efficacy of these targeted therapies (36).

In the present study, we demonstrated that ibrutinib also directly counteracted the MCL/MϕMCL dialogue through the modulation of the malignant B-cells secretome. We showed that BTK inhibition resulted in a dramatic decrease of CSF1 and IL-10 *ex vivo* and *in vivo*. Indeed, whereas higher levels of CSF1 and IL-10 were detected in the plasma of MCL compared to HD, ibrutinib treatment rapidly decreased concentrations of both cytokines. Furthermore, CD163 was overexpressed at the surface of circulating monocytes in MCL compared to HD, which was consistent with the CD163-inducing properties of CSF1 and IL-10. Of interest, the longitudinal follow up of 4 patients treated with ibrutinib highlighted a downregulation of CD163 on PB monocytes in 3 responsive patients *in vivo*. In contrast, only limited modulation was observed in the resistant patient (Pt #A9). Taken together, our results are in favor on monitoring of CSF1, IL-10 and CD163 for the follow up of patients' response to ibrutinib-based treatment. Even though a larger cohort of MCL patients treated with ibrutinib is now necessary to confirm the strength of this soluble and cellular signature, it is noteworthy that modulation of PB cytokines have also been associated to *in vivo* ibrutinib response in other B-cell malignancies(52).

Single-agent ibrutinib displayed unprecedented clinical efficacy in MCL and is now approved for use in several B-cell malignancies. Nevertheless, several mechanisms of resistance such as mutation acquisition(53), compensatory pathway activation i.e., NFκB(41) or kinome adaptive reprograming(42) have been described and retrospective studies revealed poor outcomes for ibrutinib relapsed/refractory MCL patients(54). Here we showed that targeting the CSF1R could be an alternative for disrupting the MCL/MϕMCL pro-tumoral dialogue, especially for ibrutinib-refractory patients for who poor therapeutic alternatives are available. In addition, we observed (supra)additive cytotoxicity when BTK and CSF1R inhibitors were combined at low doses *ex vivo*, suggesting that this strategy could also be beneficial for ibrutinib-sensitive patients.

In conclusion, by modeling the dialogue between MCL cells and their protective immune niches, we uncovered a novel rational combination that could overcome drug resistance. Our data reinforces the central role of the microenvironment in MCL and shows

that monocytes/macrophages are a potential target for developing novel therapeutic strategies in MCL.

Acknowledgements

This study was supported by la Ligue Contre le Cancer Grand-Ouest, i-Site NexT (ANR-16-IDEX-0007) and the SIRIC ILIAD (INCa-DGOS-Inserm_12558). We thank Janssen-Cilag and Roche for supporting in part this study. The authors thank Elise Douillard (CRCINA) for excellent technical expertise. BT is the recipient for a fellowship from Fondation ARC.

Authorship contribution

AP designed and performed experiments, analyzed data and wrote the article
BT participated in bioinformatics analysis
CB performed experiments and participated in bioinformatics analysis
AM provided biopsy samples and analyzed data
YLB provided samples
HM provided samples
PM participated in the design of the study
CT provided samples
MA participated in the design of the study and reviewed the article
CPD participated in the design of the study, in the data analysis and in the writing of the article
SLG participated in the design of the study, in the data analysis and in the writing of the article
DC designed and performed experiments, analyzed data and wrote the article

References

1. Campo E, Rule S. Mantle cell lymphoma: evolving management strategies. Blood. 2015 Jan 1;125(1):48–55.
2. Jares P, Colomer D, Campo E. Molecular pathogenesis of mantle cell lymphoma. J Clin Invest. 2012 Oct;122(10):3416–23.
3. Weisenburger DD, Armitage JO. Mantle cell lymphoma-- an entity comes of age. Blood. 1996 Jun 1;87(11):4483–94.
4. Swerdlow SH, Campo E, Pileri SA, Harris NL, Stein H, Siebert R, et al. The 2016 revision of the World Health Organization classification of lymphoid neoplasms. Blood. 2016 19;127(20):2375–90.
5. Puente XS, Jares P, Campo E. Chronic lymphocytic leukemia and mantle cell lymphoma: crossroads of genetic and microenvironment interactions. Blood. 2018 May 24;131(21):2283–96.
6. Delfau-Larue M-H, Klapper W, Berger F, Jardin F, Briere J, Salles G, et al. High-dose cytarabine does not overcome the adverse prognostic value of CDKN2A and TP53 deletions in mantle cell lymphoma. Blood. 2015 Jul 30;126(5):604–11.
7. Beà S, Valdés-Mas R, Navarro A, Salaverria I, Martín-Garcia D, Jares P, et al. Landscape of somatic mutations and clonal evolution in mantle cell lymphoma. Proc Natl Acad Sci USA. 2013 Nov 5;110(45):18250–5.
8. Queirós AC, Beekman R, Vilarrasa-Blasi R, Duran-Ferrer M, Clot G, Merkel A, et al. Decoding the DNA Methylome of Mantle Cell Lymphoma in the Light of the Entire B Cell Lineage. Cancer Cell. 2016 Nov 14;30(5):806–21.
9. Burger JA, Gribben JG. The microenvironment in chronic lymphocytic leukemia (CLL) and other B cell malignancies: insight into disease biology and new targeted therapies. Semin Cancer Biol. 2014 Feb;24:71–81.
10. Amé-Thomas P, Tarte K. The yin and the yang of follicular lymphoma cell niches: role of microenvironment heterogeneity and plasticity. Semin Cancer Biol. 2014 Feb;24:23–32.
11. Papin A, Le Gouill S, Chiron D. Rationale for targeting tumor cells in their microenvironment for mantle cell lymphoma treatment. Leuk Lymphoma. 2017 Jul 31;1–9.
12. Chiron D, Bellanger C, Papin A, Tessoulin B, Dousset C, Maiga S, et al. Rational targeted therapies to overcome microenvironment-dependent expansion of mantle cell lymphoma. Blood. 2016 15;128(24):2808–18.
13. Saba NS, Liu D, Herman SEM, Underbayev C, Tian X, Behrend D, et al. Pathogenic role of B-cell receptor signaling and canonical NF-κB activation in mantle cell lymphoma. Blood. 2016 07;128(1):82–92.
14. Chen Z, Teo AE, McCarty N. ROS-Induced CXCR4 Signaling Regulates Mantle Cell Lymphoma (MCL) Cell Survival and Drug Resistance in the Bone Marrow Microenvironment via Autophagy. Clin Cancer Res. 2016 Jan 1;22(1):187–99.
15. Chiron D, Dousset C, Brosseau C, Touzeau C, Maïga S, Moreau P, et al. Biological rational for sequential targeting of Bruton tyrosine kinase and Bcl-2 to overcome CD40-induced ABT-199 resistance in mantle cell lymphoma. Oncotarget. 2015 Apr 20;6(11):8750–9.
16. Kurtova AV, Tamayo AT, Ford RJ, Burger JA. Mantle cell lymphoma cells express high levels of CXCR4, CXCR5, and VLA-4 (CD49d): importance for interactions with the stromal microenvironment and specific targeting. Blood. 2009 May 7;113(19):4604–13.
17. Noy R, Pollard JW. Tumor-associated macrophages: from mechanisms to therapy. Immunity. 2014 Jul 17;41(1):49–61.
18. Qian B-Z, Pollard JW. Macrophage diversity enhances tumor progression and

558 metastasis. Cell. 2010 Apr 2;141(1):39–51.
559 19. Steidl C, Lee T, Shah SP, Farinha P, Han G, Nayar T, et al. Tumor-associated
560 macrophages and survival in classic Hodgkin's lymphoma. N Engl J Med. 2010 Mar
561 11;362(10):875–85.
562 20. Amin R, Mourcin F, Uhel F, Pangault C, Ruminy P, Dupré L, et al. DC-SIGN-
563 expressing macrophages trigger activation of mannosylated IgM B-cell receptor in follicular
564 lymphoma. Blood. 2015 Oct 15;126(16):1911–20.
565 21. Nguyen P-H, Fedorchenko O, Rosen N, Koch M, Barthel R, Winarski T, et al. LYN
566 Kinase in the Tumor Microenvironment Is Essential for the Progression of Chronic
567 Lymphocytic Leukemia. Cancer Cell. 2016 10;30(4):610–22.
568 22. Galletti G, Scielzo C, Barbaglio F, Rodriguez TV, Riba M, Lazarevic D, et al.
569 Targeting Macrophages Sensitizes Chronic Lymphocytic Leukemia to Apoptosis and Inhibits
570 Disease Progression. Cell Rep. 2016 Feb 23;14(7):1748–60.
571 23. Song K, Herzog BH, Sheng M, Fu J, McDaniel JM, Chen H, et al. Lenalidomide
572 inhibits lymphangiogenesis in preclinical models of mantle cell lymphoma. Cancer Res. 2013
573 Dec 15;73(24):7254–64.
574 24. Pham LV, Vang MT, Tamayo AT, Lu G, Challagundla P, Jorgensen JL, et al.
575 Involvement of tumor-associated macrophage activation in vitro during development of a
576 novel mantle cell lymphoma cell line, PF-1, derived from a typical patient with relapsed
577 disease. Leuk Lymphoma. 2015 Jan;56(1):186–93.
578 25. Hanf M, Chiron D, de Visme S, Touzeau C, Maisonneuve H, Jardel H, et al. The
579 REFRACT-LYMA cohort study: a French observational prospective cohort study of patients
580 with mantle cell lymphoma. BMC Cancer [Internet]. 2016 Oct 14;16. Available from:
581 https://www.ncbi.nlm.nih.gov/pmc/articles/PMC5064959/
582 26. Derlindati E, Dei Cas A, Montanini B, Spigoni V, Curella V, Aldigeri R, et al.
583 Transcriptomic analysis of human polarized macrophages: more than one role of alternative
584 activation? PLoS ONE. 2015;10(3):e0119751.
585 27. Murray PJ, Allen JE, Biswas SK, Fisher EA, Gilroy DW, Goerdt S, et al. Macrophage
586 activation and polarization: nomenclature and experimental guidelines. Immunity. 2014 Jul
587 17;41(1):14–20.
588 28. Maïga S, Brosseau C, Descamps G, Dousset C, Gomez-Bougie P, Chiron D, et al. A
589 simple flow cytometry-based barcode for routine authentication of multiple myeloma and
590 mantle cell lymphoma cell lines. Cytometry A. 2015 Apr;87(4):285–8.
591 29. Ritchie ME, Phipson B, Wu D, Hu Y, Law CW, Shi W, et al. limma powers
592 differential expression analyses for RNA-sequencing and microarray studies. Nucleic Acids
593 Res. 2015 Apr 20;43(7):e47.
594 30. Gautier L, Cope L, Bolstad BM, Irizarry RA. affy--analysis of Affymetrix GeneChip
595 data at the probe level. Bioinformatics. 2004 Feb 12;20(3):307–15.
596 31. Newman AM, Liu CL, Green MR, Gentles AJ, Feng W, Xu Y, et al. Robust
597 enumeration of cell subsets from tissue expression profiles. Nat Methods. 2015
598 May;12(5):453–7.
599 32. Vishwamitra D, Shi P, Wilson D, Manshouri R, Vega F, Schlette EJ, et al. Expression
600 and effects of inhibition of type I insulin-like growth factor receptor tyrosine kinase in mantle
601 cell lymphoma. Haematologica. 2011 Jun;96(6):871–80.
602 33. Baran-Marszak F, Boukhiar M, Harel S, Laguillier C, Roger C, Gressin R, et al.
603 Constitutive and B-cell receptor-induced activation of STAT3 are important signaling
604 pathways targeted by bortezomib in leukemic mantle cell lymphoma. Haematologica. 2010
605 Nov;95(11):1865–72.
606 34. Zhang L, Yang J, Qian J, Li H, Romaguera JE, Kwak LW, et al. Role of the
607 microenvironment in mantle cell lymphoma: IL-6 is an important survival factor for the tumor

cells. Blood. 2012 Nov 1;120(18):3783–92.
35. Shapouri-Moghaddam A, Mohammadian S, Vazini H, Taghadosi M, Esmaeili S-A, Mardani F, et al. Macrophage plasticity, polarization, and function in health and disease. J Cell Physiol. 2018 Sep;233(9):6425–40.
36. Mantovani A, Marchesi F, Malesci A, Laghi L, Allavena P. Tumour-associated macrophages as treatment targets in oncology. Nat Rev Clin Oncol. 2017 Jul;14(7):399–416.
37. Yeh Y-M, Hsu S-J, Lin P-C, Hsu K-F, Wu P-Y, Su W-C, et al. The c.1085A>G Genetic Variant of CSF1R Gene Regulates Tumor Immunity by Altering the Proliferation, Polarization, and Function of Macrophages. Clin Cancer Res. 2017 Oct 15;23(20):6021–30.
38. Edwards DK, Watanabe-Smith K, Rofelty A, Damnernsawad A, Laderas T, Lamble A, et al. CSF1R inhibitors exhibit anti-tumor activity in acute myeloid leukemia by blocking paracrine signals from support cells. Blood. 2018 Nov 13;
39. Bernard S, Danglade D, Gardano L, Laguillier C, Lazarian G, Roger C, et al. Inhibitors of BCR signalling interrupt the survival signal mediated by the micro-environment in mantle cell lymphoma. Int J Cancer. 2015 Jun 15;136(12):2761–74.
40. Chang BY, Francesco M, De Rooij MFM, Magadala P, Steggerda SM, Huang MM, et al. Egress of CD19(+)CD5(+) cells into peripheral blood following treatment with the Bruton tyrosine kinase inhibitor ibrutinib in mantle cell lymphoma patients. Blood. 2013 Oct 3;122(14):2412–24.
41. Rahal R, Frick M, Romero R, Korn JM, Kridel R, Chan FC, et al. Pharmacological and genomic profiling identifies NF-κB-targeted treatment strategies for mantle cell lymphoma. Nat Med. 2014 Jan;20(1):87–92.
42. Zhao X, Lwin T, Silva A, Shah B, Tao J, Fang B, et al. Unification of de novo and acquired ibrutinib resistance in mantle cell lymphoma. Nat Commun. 2017 Apr 18;8:14920.
43. Ruffell B, Affara NI, Coussens LM. Differential macrophage programming in the tumor microenvironment. Trends Immunol. 2012 Mar;33(3):119–26.
44. Hamilton JA, Cook AD, Tak PP. Anti-colony-stimulating factor therapies for inflammatory and autoimmune diseases. Nat Rev Drug Discov. 2016 29;16(1):53–70.
45. Ries CH, Cannarile MA, Hoves S, Benz J, Wartha K, Runza V, et al. Targeting tumor-associated macrophages with anti-CSF-1R antibody reveals a strategy for cancer therapy. Cancer Cell. 2014 Jun 16;25(6):846–59.
46. Zhu X-D, Zhang J-B, Zhuang P-Y, Zhu H-G, Zhang W, Xiong Y-Q, et al. High expression of macrophage colony-stimulating factor in peritumoral liver tissue is associated with poor survival after curative resection of hepatocellular carcinoma. J Clin Oncol. 2008 Jun 1;26(16):2707–16.
47. Polk A, Lu Y, Wang T, Seymour E, Bailey NG, Singer JW, et al. Colony-Stimulating Factor-1 Receptor Is Required for Nurse-like Cell Survival in Chronic Lymphocytic Leukemia. Clin Cancer Res. 2016 Dec 15;22(24):6118–28.
48. Pyonteck SM, Akkari L, Schuhmacher AJ, Bowman RL, Sevenich L, Quail DF, et al. CSF-1R inhibition alters macrophage polarization and blocks glioma progression. Nat Med. 2013 Oct;19(10):1264–72.
49. Gutiérrez-González A, Martínez-Moreno M, Samaniego R, Arellano-Sánchez N, Salinas-Muñoz L, Relloso M, et al. Evaluation of the potential therapeutic benefits of macrophage reprogramming in multiple myeloma. Blood. 2016 03;128(18):2241–52.
50. Moughon DL, He H, Schokrpur S, Jiang ZK, Yaqoob M, David J, et al. Macrophage Blockade Using CSF1R Inhibitors Reverses the Vascular Leakage Underlying Malignant Ascites in Late-Stage Epithelial Ovarian Cancer. Cancer Res. 2015 Nov 15;75(22):4742–52.
51. Priceman SJ, Sung JL, Shaposhnik Z, Burton JB, Torres-Collado AX, Moughon DL, et al. Targeting distinct tumor-infiltrating myeloid cells by inhibiting CSF-1 receptor: combating tumor evasion of antiangiogenic therapy. Blood. 2010 Feb 18;115(7):1461–71.

52. Chen JG, Liu X, Munshi M, Xu L, Tsakmaklis N, Demos MG, et al. BTKCys481Ser drives ibrutinib resistance via ERK1/2 and protects BTKwild-type MYD88-mutated cells by a paracrine mechanism. Blood. 2018 May 3;131(18):2047–59.
53. Chiron D, Di Liberto M, Martin P, Huang X, Sharman J, Blecua P, et al. Cell-cycle reprogramming for PI3K inhibition overrides a relapse-specific C481S BTK mutation revealed by longitudinal functional genomics in mantle cell lymphoma. Cancer Discov. 2014 Sep;4(9):1022–35.
54. Martin P, Maddocks K, Leonard JP, Ruan J, Goy A, Wagner-Johnston N, et al. Postibrutinib outcomes in patients with mantle cell lymphoma. Blood. 2016 Mar 24;127(12):1559–63.

691 **Figure Legends**

692 **Figure 1. Allogeneic and autologous monocytes support MCL cell survival and**
693 **promote cell proliferation.** (A) The percentage of PB MCL live cells was assessed by
694 Annexin-V staining after 7 days of culture alone (-) or with allogeneic monocytes, either in
695 contact (n = 17, left panel) or separated by transwell inserts (n = 13, right panel). Wilcoxon
696 matched pairs sign rank test. *** p < .001. Red lines represent medians. (B) Cell cycle
697 analysis (BrdU/PI) of PB MCL cells (n = 16) after 7 days of co-cultures with monocytes
698 according to their molecular subtypes (light grey: leukemic non-nodal (n = 5), dark grey:
699 conventional (n = 7), black: aggressive (n = 4)). Mann Whitney test. * p < .05. (C) Percentage
700 of live cells (AnnexinV staining, n = 4, left panel) and cell cycle analysis (BrdU/PI, n = 5, right
701 panel) of PB MCL cells cultured alone or in contact with autologous or allogeneic monocytes
702 for 7 days. Paired t-test. * p < .05 ** p < .01.
703
704 **Figure 2. MCL cells polarize monocytes into specific MϕMCL with M2-like features.** (A)
705 An ascendant hierarchical clustering was constructed with ward.D2 method of Euclidian
706 distance. M2 were generated from human monocytes cultured with CSF1/IL-10 (see
707 methods), M2' with CSF1 alone (GSE20484) and M1 with LPS/IFNg (GSE95405) (B)
708 Radarchart representation of the cibersort signature for MϕMCL and MCL-infiltrated
709 macrophages in lymph nodes. (C, left panel) CD163 Mean Fluorescence Intensity ratio
710 assessed by flow cytometry for M1 (n = 6), M2 (n = 6) and MϕMCL (n = 9) macrophages.
711 Mann Whitney test. ** p < .01 *** p < .001. (right panel) *IGF1*, *IL10* and *IL6* induction
712 measured by qRT-PCR (relative to undifferentiated human monocytes) for M1 (n = 3), M2 (n
713 = 3) and MϕMCL (n = 5) macrophages. t- test. * p < .05 ** p < .01.
714
715 **Figure 3. MCL cells express the M2-polarising factors CSF1 and IL-10.** (A) Expression of
716 *CSF1* and *IL10* in MCL cells (n = 183) compared to normal B cells (NBC, n = 15) according
717 to GEP public databases (see Methods). Mann-Whitney test. n.s, not significant. **** p
718 < .0001 ** p < .01. (B) qRT-PCR analysis of *CSF1* and *IL10* gene expression in 9 MCL cell

lines (realized in triplicate) and (C) twenty $CD19^+$ MCL samples purified from PB. Expression was normalized to Granta cell line. (D) Concentration of CSF1 and IL-10 proteins evaluated by ELISA in the supernatant of MϕMCL/MCL co-culture (7 days, n = 10). (E) Percentage of lived CD14 cells (left panel) and CD163 MFI modulation (on CD14 live cells) (right panel) after 3 days of culture with previously generated MCL/MϕMCL coculture supernatants (n = 5) in the presence of CSF1R inhibitors (GW2580 1µM, anti-CSF1R antibodies 5µg/mL), or of anti-IL-10R antibodies (5µg/mL). Paired t-test *p < .05 **p < .01 ***p < .001 (F) Percentage of primary MCL live cells in coculture with monocytes with or without GW2580 treatment (1µM) (n = 8). Cell death was assessed by Annexin-V staining. Wilcoxon matched pairs sign rank test. **p < .01. Red lines represent medians.

Figure 4. Ibrutinib counteracts MCL/MϕMCL dialogue through inhibition of CSF1. (A) qRT-PCR analysis of *CSF1* and *IL10* expression in ibrutinib-sensitive Mino cells and ibrutinib-resistant Granta cells with or without ibrutinib treatment (72h; 0.5µM). Gene expression has been normalized to the non-treated control condition of each cell line (realized in triplicate) (B) Concentration of CSF1 and IL-10 proteins evaluated by ELISA in the supernatant of Mino and Granta cells with or without ibrutinib treatment (72h; 0.5µM; triplicate). (C) (upper panel) Gating strategy to evaluate the CD163 expression on $CD14^+$ after 3 days of co-culture between monocytes and Mino or Granta cells with or without ibrutinib treatment (72h; 0.5µM) (lower panel) CD163 MFI modulation on CD14+ cells representing 3 independent experiments. (D) Percentage of primary MCL live cells in coculture with monocytes (Annexin-V staining) with or without ibrutinib treatment (72h; 0.5µM; n = 14). Wilcoxon matched pairs sign rank test. *** p < .01. (E) Cell cycle analysis (BrdU/PI) of primary MCL cells after 5 days of co-cultures with monocytes with or without ibrutinib treatment (72h; 0.5µM; n = 4). Paired t- test. *** p < .001.

Figure 5. CD163 modulation on circulating monocytes *in vivo* might be an early marker of ibrutinib response. (A) Plasma concentration of CSF1 and IL-10 proteins in MCL

patients (n = 28) and age-matched healthy donors (HD, n = 9)) by ELISA. (lower panel) Mean fluorescence intensity ratio (MFIr) of CD163 on circulating monocytes ($CD14^+$ cells) in MCL patients (n = 32) compare to age-matched HD (n = 8). Mann-Whitney test. * p < .05 ** p < .01 ***P < .001. (B) Plasma concentration of CSF1 and IL-10 and CD163 MFIr modulation on monocytes ($CD14^+$) of patient treated with anti-CD20 and ibrutinib (Clinical trial: NTC02558816). Biological parameters have been evaluated before treatment with ibrutinib and obinutuzumab (D0, black bars) and after 8 days of treatment (D8, grey bars). Variation of CD163 expression is normalized to D0 (% of D0).

Figure 6. CSF1R as a potential therapeutic target for ibrutinib resistant patients. (A) Ibrutinib-sensitive (Pt#7, 11, 15, 16) and ibrutinib-resistant (Pt#2, 5, 18, 19) primary MCL cells were cocultured with monocytes and treated with ibrutinib (0.5µM) or GW2580 (0.5µM) for 72h. (B) Ibrutinib-sensitive (Pt#7, 11, 15) and ibrutinib-resistant (Pt#5, 12, 18) primary MCL cells were cocultured with monocytes and treated with low doses of ibrutinib (125 nM) or GW2580 (125 nM) or both for 72h. Cell death was assessed by assessed by Annexin-V staining.

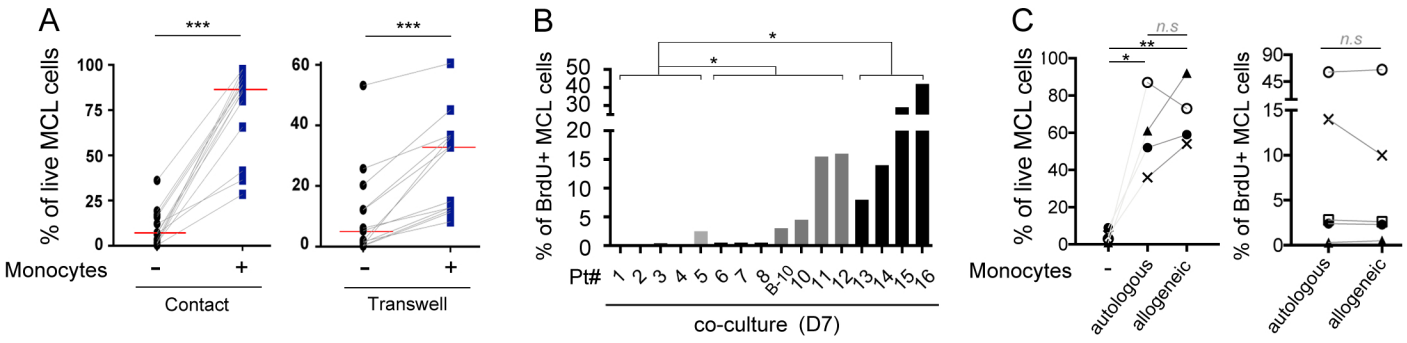

Papin et al. Figure 1

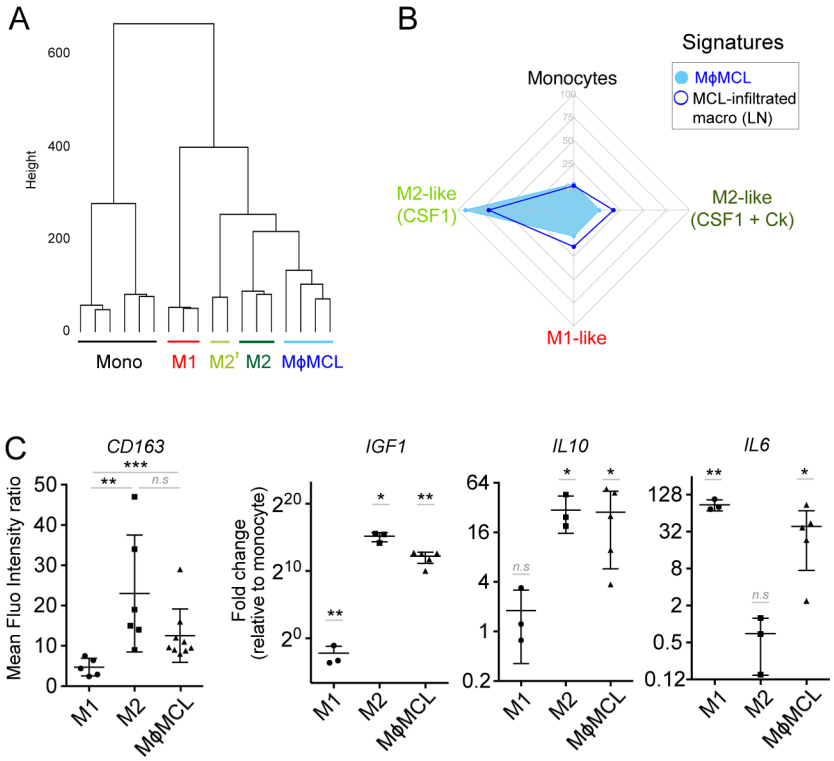

Papin et al. Figure 2

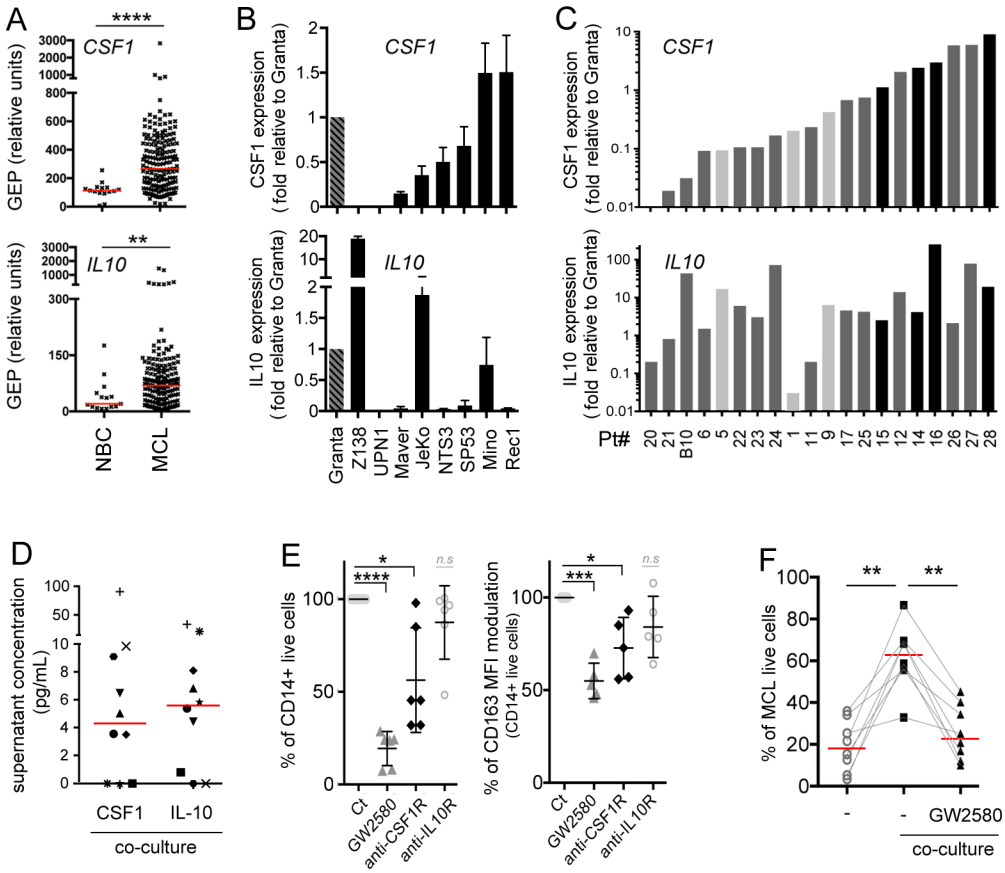

Papin et al. Figure 3

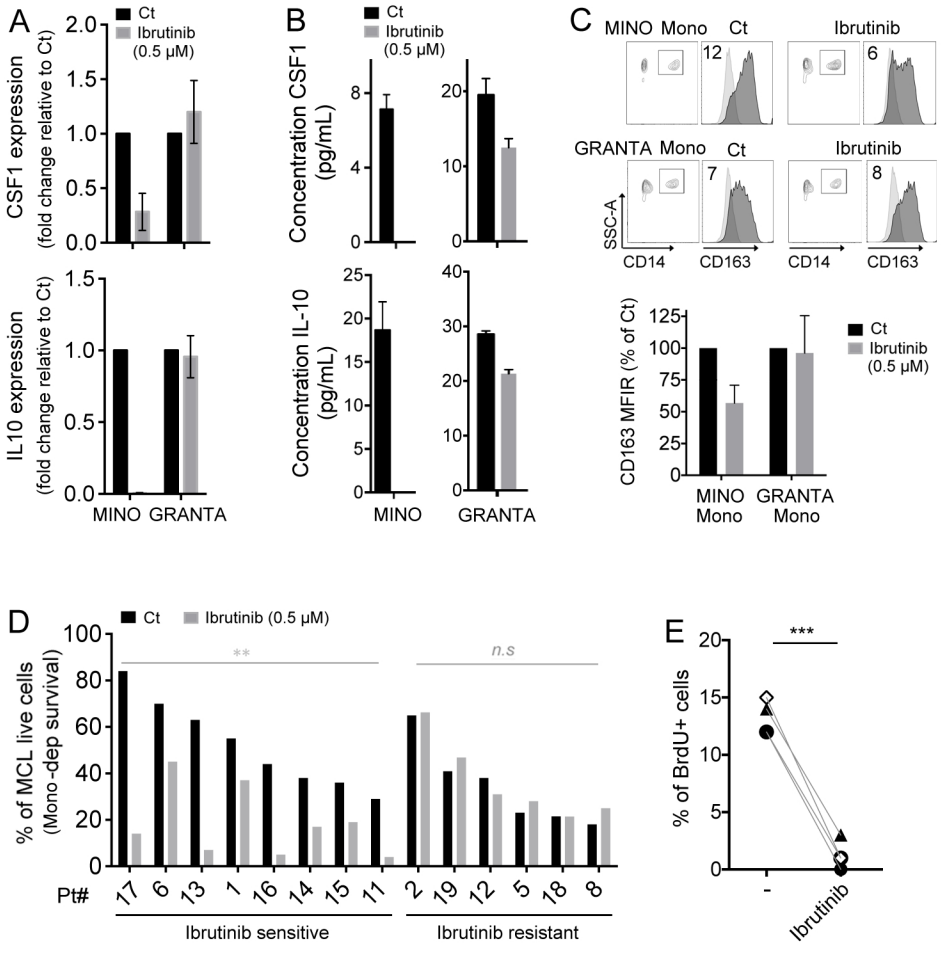

Papin et al. Figure 4

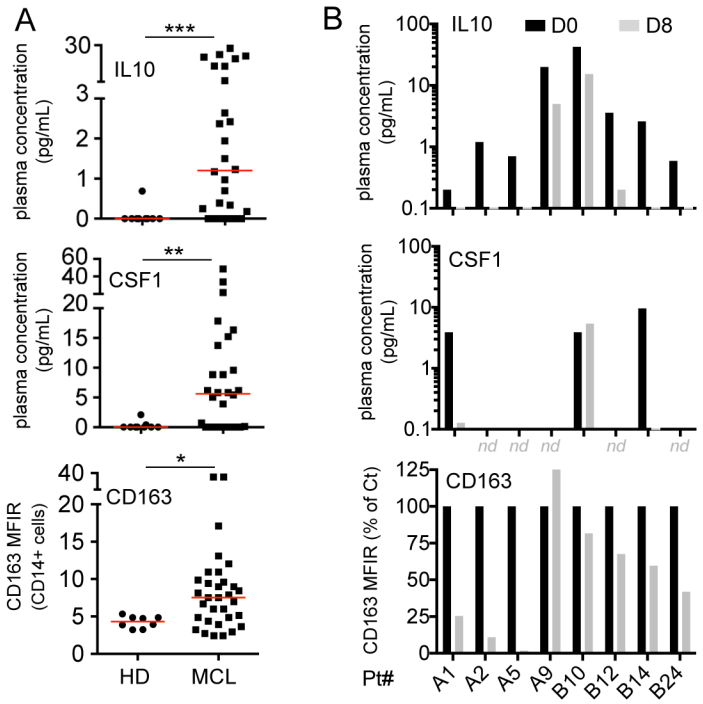

Papin et al. Figure 5

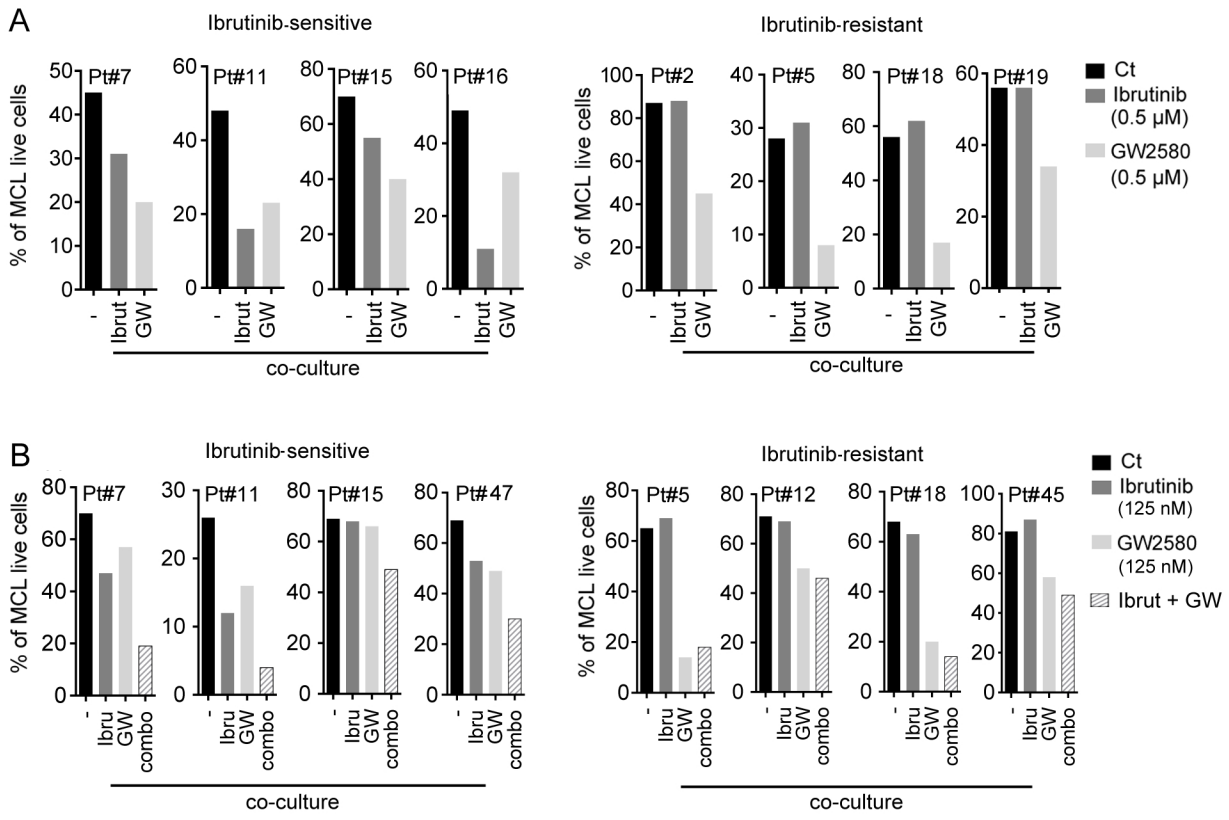

Papin et al. Figure 6